Sensors & Actuators: B. Chemical 352 (2022) 131003

Contents lists available at ScienceDirect

Sensors and Actuators: B. Chemical

journal homepage: www.elsevier.com/locate/snb

# Structured surface wetting of a PTFE flow-cell for terahertz spectroscopy of proteins

Nicholas T. Klokkou [a,b,*], David J. Rowe [b], Bethany M. Bowden [c], Neil P. Sessions [b], Jonathan J. West [d], James S. Wilkinson [b], Vasilis Apostolopoulos [a]

[a] School of Physics and Astronomy, University of Southampton, Southampton SO17 1BJ, Hampshire, United Kingdom
[b] Optoelectronics Research Centre, University of Southampton, Southampton SO17 1BJ, Hampshire, United Kingdom
[c] School of Chemistry, University of Southampton, Southampton SO17 1BJ, Hampshire, United Kingdom
[d] Faculty of Medicine, University of Southampton, Southampton SO17 1BJ, Hampshire, United Kingdom

ARTICLE INFO

*Keywords:*
Microfluidics
Terahertz spectroscopy
Protein hydration

ABSTRACT

We have fabricated a terahertz compatible polytetrafluoroethylene (PTFE) based microfluidic flow-cell, in which terahertz time-domain spectroscopy of a range of concentrations of aqueous bovine serum albumin (BSA) was performed, demonstrating the device's suitability for future studies of biomolecular interactions. The novel combination of oxygen plasma treatments and milling was used to both increase and decrease the wettability of the channel and surrounding substrate (to superhydrophobic levels) respectively, producing a stark contrast in contact angles allowing surface tension effects to confine liquid in the channel. PTFE is a chemically inert, biocompatible material with ideal spectroscopic properties at sub-millimetre wavelengths.

## 1. Introduction

Terahertz (THz) spectroscopy is a promising candidate for biomedical sensing, as large biological molecules such as proteins and nucleic acids have vibration modes on the picosecond timescale [1]. A major obstacle arises when trying to investigate these samples in their native, aqueous environment, where the highly absorbing water attenuates the THz signal. The water can be removed from the sample, either partially or entirely [2,3], or the absorption can be effectively reduced by freezing the water, shifting resonance of the molecular vibration outside of the THz range [4]. By reducing the effective thickness of the sample, however, the liquid water can be retained, representing an authentic *in vivo* protein model. In particular, the hydrogen-bond network of the surrounding water itself can be probed with THz radiation [5,6]. In this case, the influence of the protein on the surrounding solvent can be detected over greater distances than other techniques [7–10] such as nuclear magnetic resonance (NMR), with such influences on the network of bonds correlating to the macromolecules' function [11,12].

Implementing a THz compatible microfluidic device for transmission spectroscopy is an ideal solution to overcome water's strong signal attenuation, as the effective beam path-length is dramatically shortened, with added benefits such as reduced error from sample exchange and the possibility to expand such device's functionality in combination with real-time THz spectroscopy, leading to the commonly quoted term: *Lab-on-chip* [13,14]. A gas-liquid boundary in a THz compatible cell could assist in the investigation of biological processes. For example, while THz spectra of single concentrations of oxy and deoxy-hemoglobin do not show any fine spectral features in absorption in the THz band [15], changes in structure of globular proteins are detectable with THz spectroscopy by studying the effect of the macromolecule on the surrounding hydrogen bond network [16]. Differences in hydration dynamics between the two states of hemoglobin have been observed with microwave radiation [17], however, by using THz radiation instead, and by flowing oxygen and nitrogen gases adjacent to the protein solution (oxygenating and de-oxygenating the protein respectively [18,19]), the investigation of longer-range influences can be made with protein modification occurring *in situ*. Hemoglobin's function to flexibly bind and relinquish oxygen is coupled with the surrounding water network, and further investigation into its mechanism may provide greater insight into a wide range of hemoglobin disorders [20]. Furthermore, with the addition of a gas-liquid interface, such microfluidic devices can be used for the detection of airborne analytes such as drugs [21] or hazardous contaminants (ammonia) [22] by diffusion into the controlled liquid medium.

* Corresponding author at: School of Physics and Astronomy, University of Southampton, Southampton SO17 1BJ, Hampshire, United Kingdom.
*E-mail address:* ntk1g11@soton.ac.uk (N.T. Klokkou).

https://doi.org/10.1016/j.snb.2021.131003
Received 5 August 2021; Received in revised form 12 October 2021; Accepted 24 October 2021
Available online 27 October 2021

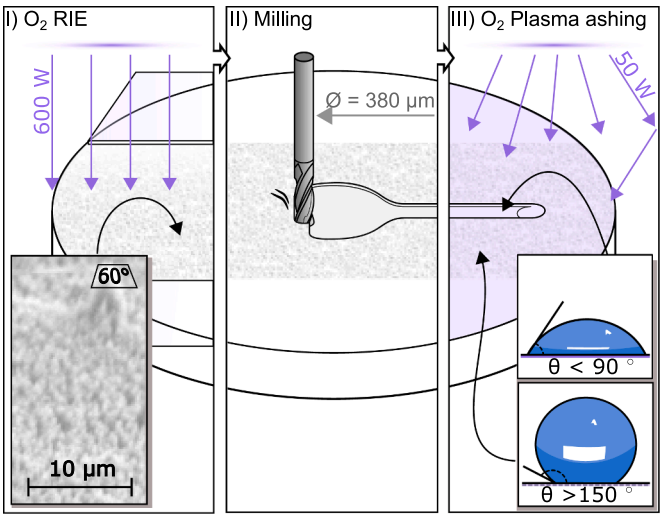


**Fig. 1.** Illustration of the microfluidic channel fabrication process, showing the stages of plasma treatment of a PTFE disc. The whole disc is first treated with reactive ion etching (RIE), creating a superhydrophobic surface. The desired channel geometry is then milled with a PCB milling machine, exposing native PTFE. The whole device is then exposed to the non-directional, $O_2$ plasma in a plasma asher where a hydrophilic channel is produced surrounded by a superhydrophobic upper surface. The leftmost insert is an image of the etched surface captured with a scanning electron microscope (SEM), with the sample tilted by 60° from the normal.

Such devices are often comprised of silicon or quartz [23,24], which have good spectroscopic properties at THz frequencies whilst benefiting from mechanical rigidity. However, specialized manufacturing processes are required to fabricate such devices, and prototyping can be slow. A faster and cheaper pathway is to use polymer based devices. Polydimethylsiloxane (PDMS) is a commonly used material in microfluidic devices; however its THz absorption characteristics are significantly dependent on its preparation methods [25]. Instead, here, we propose the use of plasma treated and machined polytetrafluoroethylene (PTFE). It has desirable properties for both use in a THz spectrometer and as a basis for a microfluidic device. Primarily, these are its low, non-dispersive refractive index between 300 GHz and 3 THz, negligible absorption over a broad THz spectrum, and its well-known chemical resistance and bio-compatibility. Whilst these attributes are appealing, two key problems emerge when trying to use PTFE for microfluidics: its lack of rigidity and the incompatibility with adhesives, complicating encapsulation methods. We aim to resolve this by producing a superhydrophobic PTFE surface which acts as a barrier to an incorporated hydrophilic channel. We show that the surface free energy contrast will enable sample confinement within the channel, bypassing the need for bonding or firmly clamping an upper substrate.

The hydrophobicity of native PTFE ($\theta_c \approx 120°$) can be both increased and decreased through plasma treatments of various powers and ionic species. High power, directional argon and oxygen plasmas can modify PTFE's surface to be superhydrophobic (contact angle, $\theta_c > 150°$) whereas a low power, ambient plasma exposure can increase the hydrophilicity of the surface [26,27], with reported contact angles as low as 40 degrees [28]. X-ray photoelectron scattering measurements have revealed that in the case of a low power exposure, it is the surface chemistry that is modified [29]. In contrast, exposure to higher energy plasmas, more specifically the accelerated particles found in reactive ion etching (RIE), changes the topology of the PTFE surface by creating significant roughness at the micro and nanoscales such that its roughness supersedes chemical effects to define a superhydrophobic surface [30].

In this paper, we exploit the surface modification of PTFE to both increase and decrease its wettability to produce a quasi-open microfluidic flow-cell, whereby confinement of aqueous samples occurs due to surface tension forces, and not from direct bonding of the substrate. We demonstrate the novel combination of RIE, machining and plasma ashing to achieve this effect, outlined in Fig. 1, allowing PTFE to be used in a sandwich scheme whereby manufacturing tolerance can be relaxed. The figure illustrates the straightforward three-step process implemented to produce a microfluidic channel with a stark contrast in contact angles between the milled channel and the surrounding substrate surface. Lastly, we show spectroscopic measurements of water and bovine serum albumin (BSA) for different concentrations in the fabricated microfluidic prototype device with a Terahertz Time-Domain Spectrometer (THz-TDS). The approach investigated exhibits the advantages of microfluidic devices where different solutions can be measured, sweeping concentrations and easily obtaining reference scans with the addition of a liquid-gas interface to enable *in situ* liquid-gas reactions to be monitored, using a material system with the chemical resistance, THz transparency, biocompatibility and hydrophobicity of PTFE. The device presented is unique in its combination of THz compatibility and provision of a liquid-gas interface, allowing application to monitoring the reaction of biological substances with gases *in situ*, as previously outlined. Additionally, this design inherently reduces the issues of bubble trapping disrupting flow and measurement, but further adds capability of the device to accept samples with dissolved gases such as carbonated drinks; the spectroscopy of which has only been achieved in unique self-referencing geometries [31] or with the implementation of nano-antennae [32].

## 2. Surface tension confinement in a THz compatible device

### 2.1. Balancing pressures for surface tension confinement

It is possible to exploit contrasts in surface wetting characteristics to make microfluidic devices that rely on capillary forces alone and no physical boundary or walls to control flow paths [33–36]. Such a scheme negates the need for problematic encapsulation by relaxing the requirement for alignment and bonding, the latter of which is particularly difficult with PTFE. Additionally, having an easily accessible liquid-gas interface allows the application of gases that may react with the liquid and/or analytes on-chip, whilst serving to help to then remove introduced air bubbles from the system.

The choice of PTFE as a material in our study liberates us from expensive fabrication techniques but at the sacrifice of having a soft material that cannot be reliably sealed by compression. This is especially true for the flow-cell dimensions needed for a THz compatible microfluidic device, motivating an alternative approach to confinement. It has been shown that selectively modifying the material surface in order to control the wetting properties of parallel coupled, etched capillaries allows for microfluidic function with a stable liquid-gas interface that relies on the Laplace pressure for confining the liquid in the channel [37]. It is feasible for this concept to be applied to the entirety of the channel, such that the principal form of confinement is from the liquid's surface tension forces. In doing so, the tolerances on device manufacturing can be relaxed, and the primary method of sealing will no longer be attributed to the elasticity of a gasket layer or by the requirement of bonding. To selectively modify the PTFE, we employ a three-stage approach as is shown in Fig. 1. In the first instance, the PTFE is plasma treated with RIE, creating a superhydrophobic surface across the entire substrate. Next, the channel is milled exposing native PTFE by completely machining the desired geometry, penetrating through the microstructured layer. Finally, the PTFE is treated by another plasma treatment, making the now exposed PTFE hydrophilic. Crucially, the last stage does not alter the initially created microstructures created, thereby maintaining superhydrophobicity. This provides a contrast in wetting characteristics for the confinement of the sample within the channel beneath an upper hydrophobic substrate contacting (but not compressed against) the modified PTFE substrate.

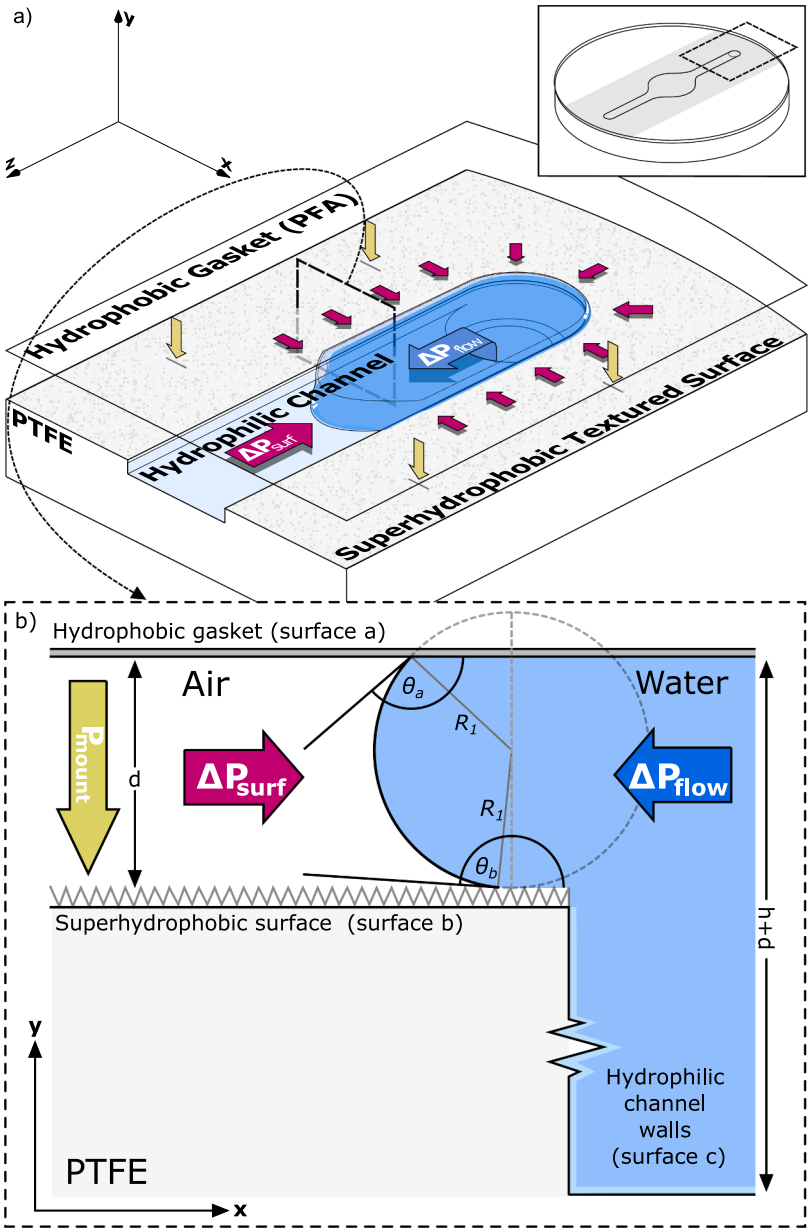


**Fig. 2.** The fundamentals of surface-tension based confinement in a microchannel. a) displays a section of straight, rectangular channel, typical of what milling the PTFE substrate will produce, with the insert illustrating the location of the cross section. The surfaces are labelled with their wettability. b) a cross section of one of the boundaries responsible for sealing the device showing the liquids meniscus with respect to the contact angles produced at the two surfaces interfaces, the geometry of which can be used to calculate the capillary pressure produced by the surface tension.

In general, for a surface of a fluid/liquid with surface tension, $\gamma$, where the curvature is defined by two radii $R_1$ and $R_2$, the difference in pressure between either side of the boundary can be expressed as [38].

$$\Delta P_{surf} = \gamma\left(\frac{1}{R_1}+\frac{1}{R_2}\right) \tag{1}$$

The concept described above is demonstrated in Fig. 2(b), in which the geometry formed from water due to its surface tension and contact angles with three types of surfaces are visualized. In this case the radius of curvature in the direction of the channel $R_2 \to \infty$ is infinite and with the geometric description shown, the radius of curvature can be given in terms of the gap between the two surfaces, $d$, which results from etching the top surface, and the contact angle at the boundary where the water meets surface $a$ and surface $b$ as $\theta_a$ and $\theta_b$ respectively. When the system is in equilibrium, this contact angle is the same as that which can be simply measured on a flat surface with a sufficiently small droplet. It then follows that Eq. (1) can then be expressed as

$$\Delta P_{surf_{ab}} = -\frac{\gamma}{d}(\cos\theta_a + \cos\theta_b) \tag{2}$$

As indicated in Fig2(b), contact angles a and b are greater than 90°, leading to a net pressure acting on the liquid resisting the filling of the space between the two materials, $d$. Similarly, this applies for the filling of the channel itself, where the pressure difference due to the upper hydrophobic substrate and the channel base, $\Delta P_{Surf\,ac}$, can be calculated by

$$\Delta P_{surf_{ac}} = -\frac{\gamma}{h+d}(\cos\theta_a + \cos\theta_c) \tag{3}$$

where the total space between the two surfaces now includes the channel depth, $h$. Therefore, we can see that to reduce back-pressure we would rather reduce the contact angle of the channel surface. Indeed, if the contact angle of just the channel surface is sufficiently reduced, capillary action will cause the channel to be self-wetting. It is evident that being able to localize surface modification to increase or decrease contact angles would be beneficial to aid confinement on filling or reintroduction of new liquids.

Once the channel has been completely wetted, for a wide channel ($w >> h$) the maximum pressure difference required for fluid flow,

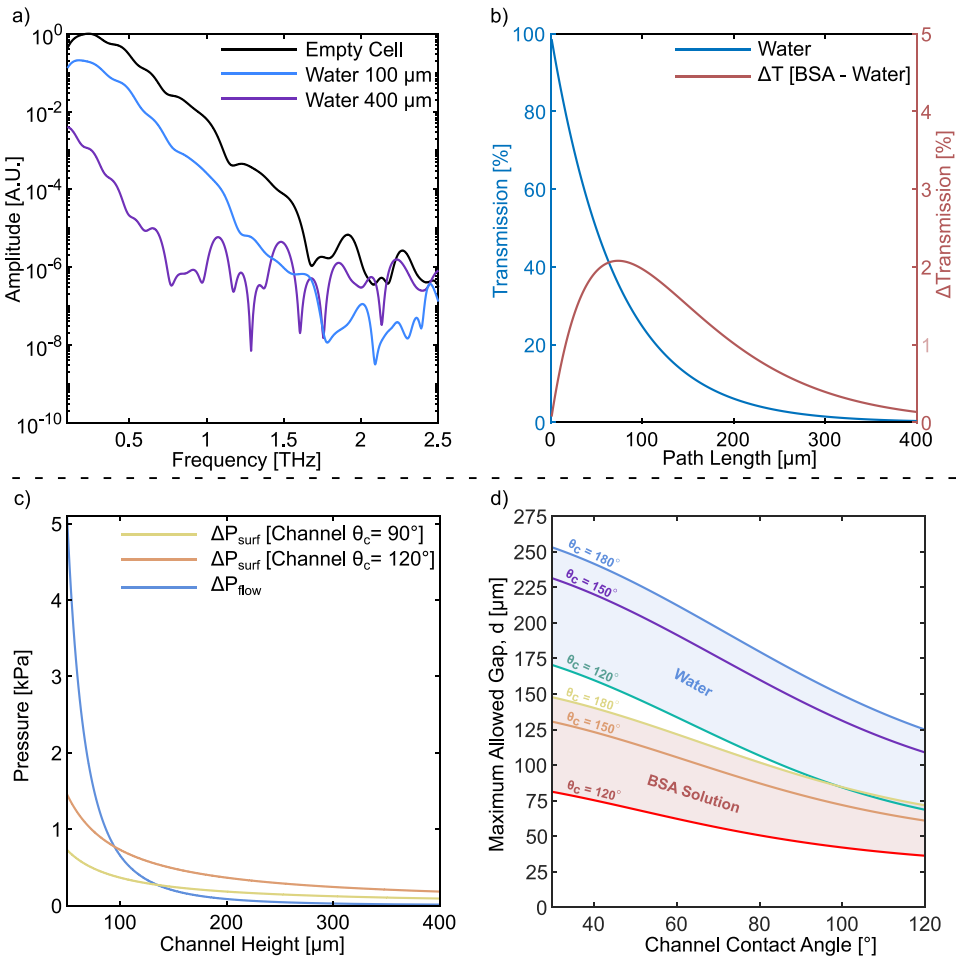


**Fig. 3.** a) THz transmission frequency spectra of an empty PTFE flow-cell, 100 μm and 400 μm of water. b) Transmission of 500 GHz radiation through water of increasing depth up to 400 μm (blue) and delta transmission between water and 33 mg/mL of BSA solution (red). c) Back pressures caused by filling the channel against channel height, for a channel contact angle of 90° (yellow), 120° (orange) where the cap has a contact angle of 120° in both cases. The pressure difference required for a steady flow in a 1.6 mm wide channel is calculated (blue). d) Theoretical maximum gap for surface tension confinement of water (blue) and a 100 mg/mL BSA solution (red), where the gap required is plotted against the contact angle of the surface in a 100 μm deep, 1.6 mm wide channel, for a range of contact angles of the upper surface, with three key values plotted as lines: 120°, for native PTFE, 150°, what was measurable for the superhydrophobic surface, and 180°, the absolute upper limit. For BSA solution, approximations for viscosity η were taken to be twice that of water and surface tension, γ, to be two thirds of that of water. Values obtained by numerically solving Eq. (5) for gap, d.

$\Delta P_{flow}$, for a flow-rate $Q$, is given by [38]:

$$\Delta P_{flow} = \frac{12\eta LQ}{(h+d)^3 w[1-0.63\frac{h+d}{w}]} \tag{4}$$

where the channel length $L$ and fluid of viscosity $\eta$ contribute proportionally. For confinement to occur, the pressures responsible for retaining the liquid in the channel must be greater than those responsible for expelling it. Therefore, the condition for confinement can be expressed as

$$\Delta P_{surf_{ab}} - \Delta P_{surf_{ac}} - \Delta P_{flow} - \Delta P_{hydro} > 0 \tag{5}$$

The additional term, $\Delta P_{hydro}$, that is included in this expression is the hydrostatic pressure caused by height difference in the medium and the density of the fluid. In microfluidics this is often ignored, especially in horizontal configurations or when the device is completely, physically sealed. However, we cannot ignore such a term in the case of a surface tension confined, vertically orientated device, of which is a desirable configuration for aligning horizontal beam paths of our spectrometer. Here, we note that $\Delta P_{flow} \propto h^{-3}$ and $\Delta P_{flow} \propto Q$ as our requirement is to minimize $h$ for optimum THz wave transmission, meaning that in doing so we increase the confinement pressures required. While the flow rate can be simply reduced to mitigate leaking, we found that we have practical lower limits for $Q$ as too little flow increases the likelihood of air bubble trapping and poor displacement of previous liquid samples, compromising one of the benefits of microfluidic devices: reliable automation.

### 2.2. Optimizing design for both THz spectroscopy and surface tension confinement

For a THz compatible device, the height of the channel greatly affects the resulting available bandwidth and sensitivity of detected radiation in transmission. Fig. 3(a) shows a typical spectrum of our THz spectrometer through an empty PTFE flow-cell, with 100 μm and 400 μm thicknesses of water measured in earlier prototype devices. The bandwidth and peak signal-to-noise ratio of a single THz pulse frequency spectrum is significantly reduced with increasing path length. Of course, an increase in path length will increase sensitivity to a change in the absorbing medium. By using the measured absorption coefficients for a BSA solution of 33 mg/mL [39] and that of water [40], a calculation of transmission with varying thicknesses can be made. We choose to define sensitivity by subtracting the two theoretical transmissions for different thickness to estimate at which path length the maximum difference, indicated in Fig. 3(b), where a peak delta in transmission occurs just below 100 μm of water, indicating that for both retention of signal strength and for sensitivity, a channel depth of 100 μm should be targeted.

The implications on of reducing the channel height of a 1.6 mm wide channel are explored in Fig. 3(c). Eq. (3) was used to calculate the Laplace pressures that arise when filling both a treated ($\theta_c = 90°$) and untreated ($\theta_c = 120°$) PTFE channel, with increasing channel height. Additionally, Eq. (4) was used to calculate the pressure difference required for a constant flow rate of 50 μL/min, again with varying channel height. The sum of the Laplace and fixed flow rate pressure drops shown in this figure act against the confinement of our device. The contribution from the fixed flow rate becomes the dominant term below

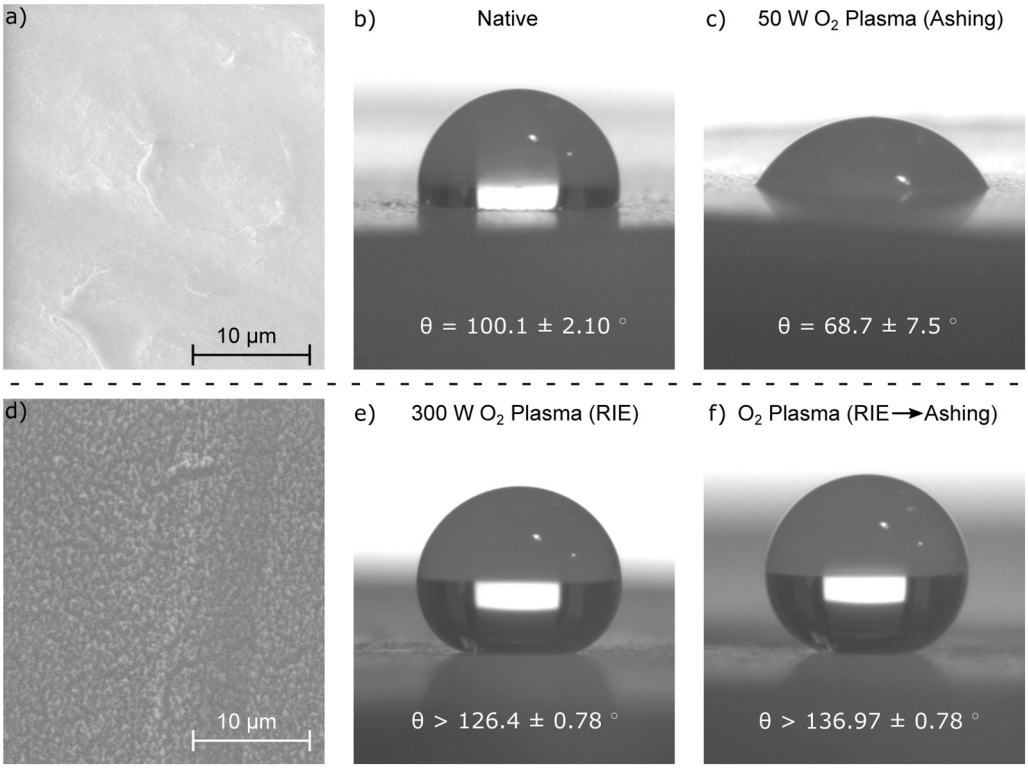


**Fig. 4.** Examples of images used for contact angle measurements proceeded by SEM images of plasma modified PTFE. All droplets have a volume of 20 μm, as this was the minimum volume size required for the water to leave the needle. a) SEM image of untreated PTFE, showing typical native surface, b) Image of water on an untreated PTFE substrate, c) a substrate after $O_2$ plasma ashing, clearly showing hydrophilic behaviour, d) SEM image of PFTE after the RIE treatment, e) attempt at contact angle measurement of PTFE after 30 min of RIE treatment. Droplet migrated to a stable point where captured contact angle is lower than that typical of a smooth surface. f) is an attempt to measure the contact angle of PTFE after RIE and then the ashing process, but the etched surface roughness causes the surface to retain superhydrophobicity. Similarly to e), the drop still moved to a defect on the disc and measured angles from this image will be an underestimate. f) A sharp increase in surface roughness indicates the cause for the superhydrophobic behaviour.

channel heights of 100 μm, and sharply increases as it is reduced. By implementing a simple Newton-Raphson method, Eq. (5) can be solved for the maximum allowed gap for confinement, $d_{max}$, for varying channel contact angle and repelling surface contact angle, the results of which are shown in Fig. 3(d). Aqueous protein solution typically has a reduced surface tension and increased viscosity. To indicate such effects on confinement criteria, we picked parameters that roughly coincide with 100 mg/mL BSA solution, a very high concentration, but not unheard of in THz spectroscopy analysis. A solution of this concentration has a viscosity, $\eta_{BSA} \approx 2\ mPa\ s$ [41] (as opposed to water, $\eta_{water} = 1\ mPa\ s$), and we take an approximate surface tension, $\gamma_{BSA} \approx 50$ mN/m (opposed to water, $\gamma_{water} = 72.8$ mN/m) [42].

While the tolerance for leaking due to gap sizes for high concentrations of protein decrease, the effect can be entirely accounted for with surface modifications. Confinement is maintained with an achievable 90° channel contact angle and a 150° repelling surface contact angle, with much greater enhancement as the channel and repelling surfaces are made hydrophilic and superhydrophobic respectively. Such an increase in tolerance to defect induced leaking allows PTFE to be used in a for THz compatible device (100 μm thickness) as the contact angle contrast will confine liquids of higher viscosity than water at the same flow rate.

## 3. Methods, results and discussion

### 3.1. Surface modification of PTFE

To modify the surface chemically, such that it becomes hydrophilic, PTFE discs parted from an extruded rod were treated with oxygen plasma in a plasma asher for three minutes at a 50 W power setting, at maximum flow-rate, selected from a parameter sweep where higher or lower values reduced the wetting effect. The contact angle of the treated surface reduced from a measured 100.1 ± 2.1° to 68.7 ± 7.5° as can be seen in Fig. 4(b) and (c) respectively, with (a) showing a scanning electron microscope (SEM) image (taken in partial vacuum) of an untreated, PTFE surface. Physio-chemical surface modification is expected to change over time [43] however aging with the PTFE exposed to water is far slower than in air, and the hydrophilicity can possibly be rejuvenated. We predict that with regular use in a microfluidic device the reduced contact angle of these surfaces will remain stable, however, with the subsequently described treatment, the device will still be able to confine most aqueous samples if the channel's wettability fails over said long period. A superhydrophobic surface was created by etching micro-structures with RIE with oxygen species. If the surface tension is high enough such that the liquid bridges over the microscopic valleys of the structures, the contact angle is enhanced to become an effective contact angle. This is a function of the Young's contact angle, $\theta$, of the unmodified material and that of air present in the valleys of the structures. When this occurs, the system is said to be in the Cassie-Baxter state [44].

$$\cos\theta_{CB} = f_1 \cos\theta - f_2 \tag{6}$$

where $f_1$ and $f_2$ are fractions of solid/liquid and air/liquid of the effective surface respectively. It can be seen from this equation that whilst the measured Cassie-Baxter contact angle $\theta_{CB}$ does indeed depend on the material's surface Young's contact angle, $\theta_{CB}$ will still show an enhancement even in the case of a hydrophilic substrate. To achieve a sufficiently rough topology, the PTFE was treated for 30 min with RIE (300 W, 5 sccm of $O_2$, 50 mTorr, 600 V DC bias produced). Contact angle measurements show that the surface was superhydrophobic. However, it was not possible to obtain a reliable measurement, as the water droplet resisted leaving the deposition needle, requiring a larger droplet size to be effectively deposited. The water then accelerated away from the target and came to rest at a defect, with the image of the droplet in Fig. 4(d). The measurements made at this point will be an underestimate, so we can only report contact angle enhancement of $\theta_{CB} > 126.4 \pm 0.78°$. Observation under an SEM shows the topological result of the treatment in Fig. 4(f) where a high degree of roughness is visible. Additionally, the roughness can be seen with the naked eye as a matting of the otherwise slightly glossy PTFE surface.

Eq. (6) suggests that if the fraction of air to the material surface is

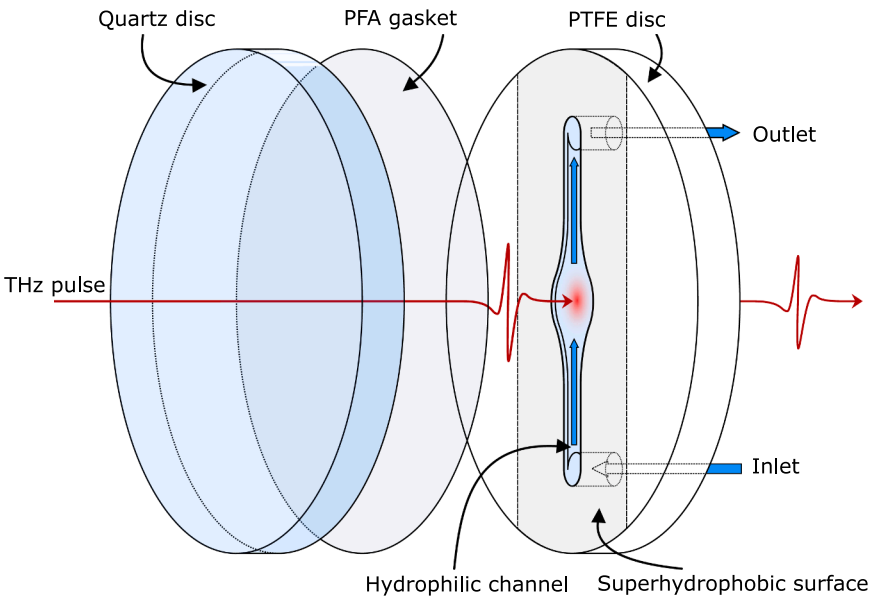


**Fig. 5.** The geometry and core components of the microfluidic flow-cell. A microfluidic channel with a 6 mm wide zone for the transmission of the THz beam is machined into a 5 mm thick, 50 mm diameter PTFE disc by a PCB milling machine. Assembly pressure provided by a 3D printed manifold (not shown) lightly contacting a 5 mm thick, 50 mm diameter quartz disc and 50 μm thick PFA gasket on top of the device. The 1.6 mm inlet holes were introduced using the same PCB milling machine.

high enough, then the contact angle will increase even if the case of lower Young's contact angles. By exposing an already etched substrate of PTFE to the $O_2$ plasma from the plasma asher, the surface roughness contribution to the effective contact angle supersedes the effect of the chemical change and the surface remains superhydrophobic, as evident in Fig. 4(e). Indeed, this was the case as it was similarly difficult to quantify what the contact angle was as with just the RIE exposure alone: $\theta_{CB} > 136.97 \pm 0.78°$. With these methods, we can easily create a high contrast in wettability without the need for a mask, by first treating a PTFE substrate with RIE, milling the desired geometry (exposing unaltered, native PTFE), and then treating the whole substrate in a plasma asher. After doing so the milled channel will be relatively hydrophilic whereas the upper, micro-structured surfaces will continue to be superhydrophobic.

### *3.2. THz spectra of aqueous protein solutions using the surface-modified PTFE flow-cell*

The key components of the fabricated final device are outlined in Fig. 5. A 50 mm diameter, 5 mm thick PTFE disc was treated with the RIE process previously described. During the RIE process two glass slides were used to mask the edges of the material, producing a step down to the superhydrophobic micro-structured area and protects this area from being damaged by contact when the device is assembled. The channel geometry and inlet holes were milled and drilled respectively on a PCB milling machine (LPKF ProtoMat s64) with a 380 μm diameter mill tool and a 1.6 mm diameter drill tool. The inlet channel width was chosen to match the 1.6 mm inlet holes both to minimize required pressures for steady flow while also allowing for opportunity for smooth transitions between milled and drilled areas on the substrate. The substrate was sonicated in isopropyl alcohol and de-ionised water each for ten minutes to remove any machining fragments and residue from handling. The whole substrate was exposed to the $O_2$ plasma treatment outlined previously, reducing the contact angle of the newly exposed PTFE in the channel. For enclosing the device, a z-cut quartz disc of 50 mm diameter and 5 mm thickness was chosen for its THz and optical transparency to visually inspect the flow in the device. A 50 μm thick tetrafluoroethyleneperfluoro(alkoxy vinyl ether) (PFA) gasket layer with a hydrophobic surface (and similar THz spectroscopic characteristics to PTFE) was used to enclose the channel. It is possible for another PTFE disc to be used instead of quartz and PFA if visual inspection is not needed. Substituting PTFE would reduce reflection losses and simplify the device further. The assembly does not require a large compression force to provide a seal as we rely on surface tensions forces only. As such, a simple 3D printed manifold was used enabling faster prototyping than the large, metallic manifold that has previously been required for a similar scheme (without the surface modification) for microwave resonance spectroscopy [45]. Avoiding metallic elements has the addition benefit of making the device lighter and easier to align vertically in our time-domain spectrometer. Each of the processes implemented here are well established and widely available. Furthermore, the simplicity of each step suggests potential for scaling-up manufacturing in a cost-effective manner.

The assembled device accepts water and more viscous protein solutions at the same flow rate, with the added benefit of removing any air bubbles introduced by syringe exchange. As well as tolerating air introduction, this also demonstrates the sealing of the device being due to surface tension forces, as a gas-liquid interface must be present. Complete replacement of even the more viscous samples was confirmed with visual inspection, where dyed high- concentrations of BSA solution (100 mg/mL) could be seen to be completely replaced by DI water through visual inspection through the quartz disc. The dye used (Tripan Blue, Sigma Aldrich) is potent enough that any residue would be visible through a slow colour transition rather than a smooth, advancing boundary.

Our THz-TDS is driven by a Ti:Sapphire mode-locked laser, which outputs 100 fs pulses at 780 nm peak wavelength, incident on photoconductive antennae emitters and detectors. A delay is introduced to the pulses incident on the emitter by a high speed delay line. The emitted THz broadband pulse is collimated and focused through the centre of the flow-cell, then recollimated and subsequently focused onto the detector. The THz components are housed in an aluminium box which is purged with nitrogen gas to remove water vapour absorption lines.

Lyophilized BSA powder (Sigma A7906) 98% purity was weighed and mixed with de-ionized water, then sonicated for 10 min. Each concentration was introduced to the cell *via* a syringe pump and a PTFE inlet tube at a flow of 50 μL/min. Initially, a time-domain transmission spectrum of the empty cell was measured and then starting with water, each new solution was passed through, and two-minute-long scans were recorded to get a THz spectrum. The spectrum of each solution was divided by the reference spectrum (the empty cell) to obtain an experimental transfer function; the complex refractive index was extracted by fitting a theoretical transfer function to the data using the Newton-Raphson method. All data has been windowed in the time-domain to

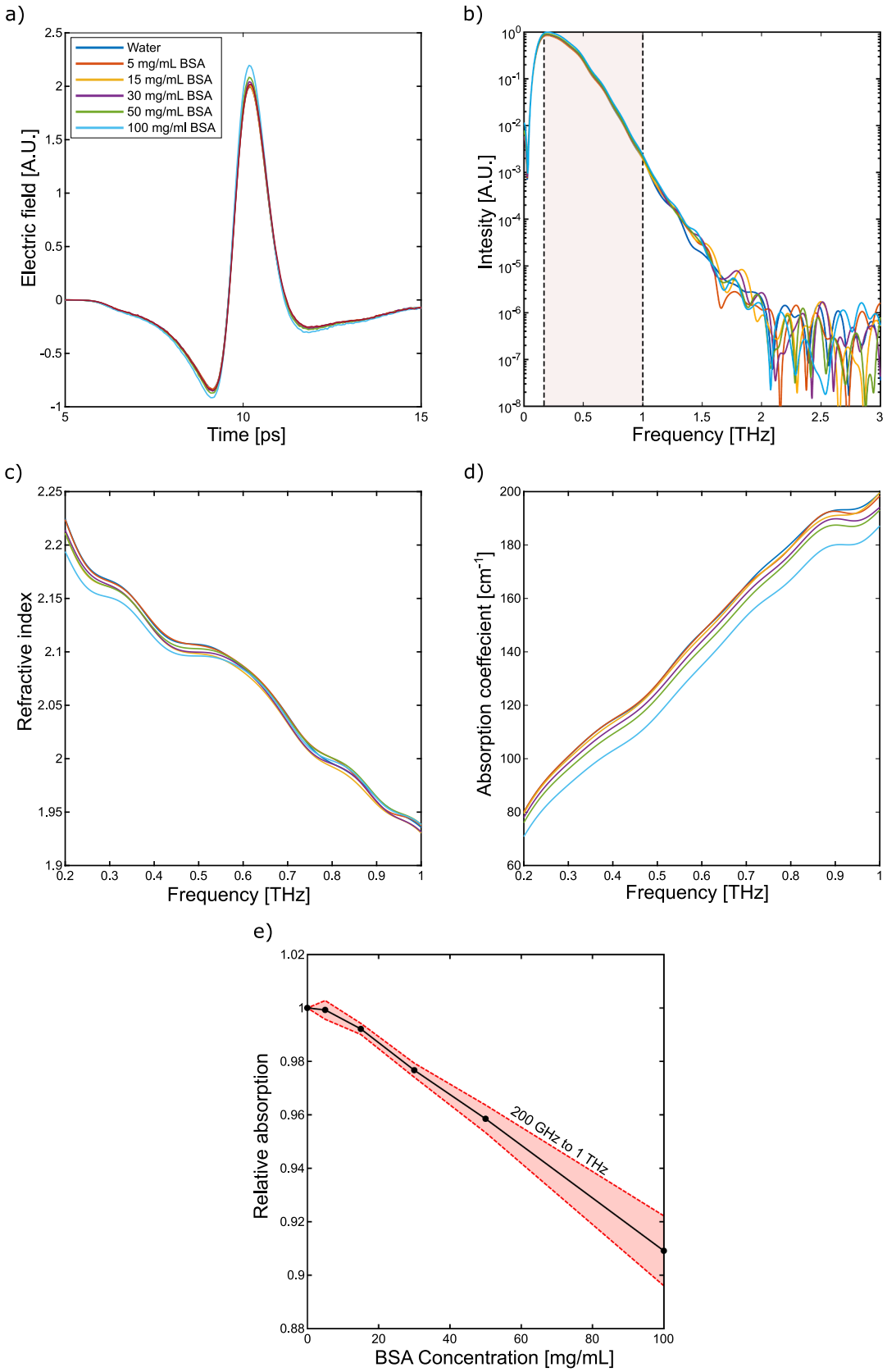


**Fig. 6.** THz-TDS scans and extracted parameters for water and aqueous BSA concentrations up to 100 mg/mL. The time domain pulses (a) and the associated frequency spectra (b). Focusing on a range of 200 GHz to 1 THz, the extracted refractive index (c) and absorption coefficient (d) are shown, with small variations due to protein concentration. By calculating the relative absorption by division of the measured water absorption for each frequency, the average relative absorption for each concentration (black circles) is plotted with the standard deviation (dotted red) to show the spread across frequencies.

remove reflections and to allow for simpler fitting.

Fig. 6 shows the terahertz scans of the water and BSA solutions. By looking purely at the time-domain and frequency-domain spectra (Fig. 6 (a) and (b) respectively). The small path length of the microfluidic channel allows for a wide bandwidth of THz spectra to remain above the noise floor. The small differences in frequency dependent complex refractive indices between the samples are not obvious, as attenuation of signal can be from both reflections dominated by the real refractive index as well as absorption directly from the extinction coefficient. Extracting the real refractive index and the absorption coefficient (Fig. 6 (c) and (d) respectively) confirms that the most significant contribution on signal change due to presents of BSA protein is the absorption coefficient, where only comparably small changes in the real refractive index are visible. The relative absorption was calculated by dividing each frequency dependent absorption coefficient for BSA concentrations by the measured water absorption. Oscillations in the frequency domain are present due to the window function applied (Tukey), however do not affect the differential measurements with respect to water. The average of this was made over the 200 GHz and 1 THz frequency range which is shown, along with the standard deviation, is shown in Fig. 6. As mentioned in the introduction, a key area of interest is the terahertz response of protein hydration and dynamic water bond networks. A non-linear trend in the concentration dependent absorption coefficient indicates the presence of a third component (in addition to protein and bulk water volume): hydration shell water. As observed in Refs. [5–12], the trend is not what would be expected in the case of the simple exchange of water with protein volume but evidences the introduction of a third component relating to the hydration shell.

## 4. Conclusion

A PTFE flow-cell for terahertz spectroscopy of biological media has been demonstrated in this work. PTFE offers low absorption at THz frequencies and the low surface free energy characteristic of PTFE produces a non-fouling and bio-compatible surface, desirable for many microfluidic applications. However, this characteristic hampers efforts for bonding and encapsulating the microfluidic channels. New encapsulation approaches are therefore required for the effective implementation of PTFE in microfluidics, and here we have demonstrated a cost effective and robust solution. A novel combination of plasma treatments of PTFE to provide a strongly localized contrast in wetting characteristics on a single substrate has been demonstrated. This leads to realization of a flow-cell with optimized path-length of aqueous media that exploits surface tension forces to achieve easy confinement of the liquid medium, enabling THz spectroscopic measurements of aqueous solutions of biological macromolecules. The cell is demonstrated for THz spectroscopy of aqueous solutions of the common model protein bovine serum albumin determining the complex refractive index and hence absorption coefficient as a function of both frequency and BSA concentration. The straightforward fabrication process will allow for rapid prototyping and customization for further development of device functionality, and the gas-liquid interface inherent to the confinement method provides an excellent platform for future study of the effects of gas interactions on protein hydration, such as hemoglobin oxygenation, potentially allowing for the detection of small changes in conformation of gas-sensitive proteins with the reaction being performed ‘on-chip’.

## Funding

This work was funded by EPSRC *via* a Ph.D. studentship for N.T. Klokkou. Additionally, Bethany Bowden thanks the Defence Science and Technology Laboratory (Contract no. DSTLX-1000128554) for supporting an EPSRC industrial CASE student award.

## CRediT authorship contribution statement

**Nicholas T. Klokkou:** Conceptualization, Investigation, Methodology, Software, Formal analysis, Validation, Writing – original draft, Visualization. **David J. Rowe:** Conceptualization, Writing – review & editing. **Bethany M. Bowden:** Investigation, Formal analysis, Writing – review & editing. **Neil P. Sessions:** Investigation. **Jonathan J. West:** Investigation, Writing – review & editing. **James S. Wilkinson:** Supervision, Writing – review & editing. **Vasilis Apostolopoulos:** Supervision, Writing – review & editing.

## Declaration of Competing Interest

The authors declare that they have no known competing financial interests or personal relationships that could have appeared to influence the work reported in this paper.

## References

[1] P.U. Jepsen, D.G. Cooke, M. Koch, Terahertz spectroscopy and imaging – modern techniques and applications, Laser Photonics Rev. 5 (1) (2011) 124–166, https://doi.org/10.1002/lpor.201000011.
[2] C. Zhang, E. Tarhan, A.K. Ramdas, A.M. Weiner, S.M. Durbin, Broadened far-infrared absorption spectra for hydrated and dehydrated myoglobin, J. Phys. Chem. B 108 (28) (2004) 10077–10082, https://doi.org/10.1021/jp049933y.
[3] A.G. Markelz, A. Roitberg, E.J. Heilweil, Pulsed terahertz spectroscopy of DNA, bovine serum albumin and collagen between 0.1 and 2.0 THz, Chem. Phys. Lett. 320 (1–2) (2000) 42–48, https://doi.org/10.1016/s00092614(00)00227-x.
[4] A.G. Markelz, J.R. Knab, J.Y. Chen, Y. He, Protein dynamical transition in terahertz dielectric response, Chem. Phys. Lett. 442 (4–6) (2007) 413–417, https://doi.org/10.1016/j.cplett.2007.05.080.
[5] U. Heugen, G. Schwaab, E. Brϋndermann, M. Heyden, X. Yu, D.M. Leitner, M. Havenith, Solute-induced retardation of water dynamics probed directly by terahertz spectroscopy, Proc. Natl. Acad. Sci. USA 103 (33) (2006) 12301–12306, https://doi.org/10.1073/pnas.0604897103.
[6] S. Ebbinghaus, J.K. Seung, M. Heyden, X. Yu, U. Heugen, M. Gruebele, D. M. Leitner, M. Havenith, An extended dynamical hydration shell around proteins, Proc. Natl. Acad. Sci. USA 104 (52) (2007) 20749–20752, https://doi.org/10.1073/pnas.0709207104.
[7] M. Heyden, E. Brϋndermann, U. Heugen, G. Niehues, D.M. Leitner, M. Havenith, Long-range influence of carbohydrates on the solvation dynamics of water – answers from terahertz absorption measurements and molecular modeling simulations, J. Am. Chem. Soc. 130 (17) (2008) 5773–5779, https://doi.org/10.1021/ja0781083.
[8] B. Born, S.J. Kim, S. Ebbinghaus, M. Gruebele, M. Havenith, The terahertz dance of water with the proteins: the effect of protein flexibility on the dynamical hydration shell of ubiquitin, Faraday Discuss. 141 (2009) 161–173, https://doi.org/10.1039/B804734K.
[9] O. Sushko, R. Dubrovka, R.S. Donnan, Sub-terahertz spectroscopy reveals that proteins influence the properties of water at greater distances than previously detected, J. Chem. Phys. 142 (5) (2015), 055101, https://doi.org/10.1063/1.4907271.
[10] D.M. Leitner, M. Gruebele, M. Havenith, Solvation dynamics of biomolecules: modeling and terahertz experiments, HFSP J. 2 (6) (2008) 314–323, https://doi.org/10.2976/1.2976661.
[11] K. Meister, S. Ebbinghaus, Y. Xu, J.G. Duman, A. Devries, M. Gruebele, D. M. Leitner, M. Havenith, Long-range protein-water dynamics in hyperactive insect antifreeze proteins, Proc. Natl. Acad. Sci. USA 110 (5) (2013) 1617–1622, https://doi.org/10.1073/pnas.1214911110.
[12] B. Born, H. Weingärtner, E. Brϋndermann, M. Havenith, Solvation dynamics of model peptides probed by terahertz spectroscopy. Observation of the onset of collective network motions, J. Am. Chem. Soc. 131 (10) (2009) 3752–3755, https://doi.org/10.1021/ja808997y.
[13] P.A. George, W. Hui, F. Rana, B.G. Hawkins, A.E. Smith, B.J. Kirby, Microfluidic devices for terahertz spectroscopy of biomolecules, Opt. Express 16 (3) (2008) 1577–1582, https://doi.org/10.1364/oe.16.001577.
[14] L. Liu, R. Pathak, L.J. Cheng, T. Wang, Real-time frequency-domain terahertz sensing and imaging of isopropyl alcohol-water mixtures on a microfluidic chip, Sens. Actuators B: Chem. 184 (2013) 228–234, https://doi.org/10.1016/j.snb.2013.04.008.
[15] S. Nagatomo, K. Saito, K. Yamamoto, T. Ogura, T. Kitagawa, M. Nagai, Heterogeneity between two α subunits of $\alpha_2\beta_2$ human hemoglobin and $O_2$ binding properties: Raman, $^1$H nuclear magnetic resonance, and terahertz spectra, Biochemistry 56 (46) (2017) 6126–6136, https://doi.org/10.1021/acs.biochem.7b00733.
[16] Y. Sun, J. Zhong, C. Zhang, J. Zuo, E. Pickwell-MacPherson, Labelfree detection and characterization of the binding of hemagglutinin protein and broadly neutralizing monoclonal antibodies using terahertz spectroscopy, J. Biomed. Opt. 20 (3) (2015), 037006, https://doi.org/10.1117/1.jbo.20.3.037006.

[17] L. Latypova, G. Barshtein, A. Puzenko, Y. Poluektov, A. Anashkina, I. Petrushanko, S. Fenk, A. Bogdanova, Y. Feldman, Oxygenation state of hemoglobin defines dynamics of water molecules in its vicinity, J. Chem. Phys. 153 (13) (2020), 135101, https://doi.org/10.1063/5.0023945.
[18] S. Longeville, L.R. Stingaciu, Hemoglobin diffusion and the dynamics of oxygen capture by red blood cells, Sci. Rep. 7 (1) (2017) 1–10, https://doi.org/10.1038/s41598-017-09146-9.
[19] K.Z. Chng, Y.C. Ng, B. Namgung, J.K.S. Tan, S. Park, S.L. Tien, H.L. Leo, S. Kim, Assessment of transient changes in oxygen diffusion of single red blood cells using a microfluidic analytical platform, Commun. Biol. 4 (1) (2021) 1–10, https://doi.org/10.1038/s42003-021-01793-z.
[20] B.G. Forget, H. Franklin Bunn, Classification of the disorders of hemoglobin, Cold Spring Harb. Perspect. Med. 3 (2) (2013) 1–12, https://doi.org/10.1101/cshperspect.a011684.
[21] T. Frisk, D. Rönnholm, W. Van Der Wijngaart, G. Stemme, A micromachined interface for airborne sample-to-liquid transfer and its application in a biosensor system, Lab Chip 6 (12) (2006) 1504–1509, https://doi.org/10.1039/b612526n.
[22] J.D. Greenwood, Y. Liu, D.E. Busacker, D. Cheng, H. Jiang, Collection of gaseous and aerosolized samples using microfluidic devices with gas-liquid interfaces, IEEE Sens. J. 10 (5) (2010) 952–959, https://doi.org/10.1109/JSEN.2009.2038071.
[23] X. Hu, G. Xu, L. Wen, H. Wang, Y. Zhao, Y. Zhang, D.R. Cumming, Q. Chen, Metamaterial absorber integrated microfluidic terahertz sensors, Laser Photonics Rev. 10 (6) (2016) 962–969, https://doi.org/10.1002/lpor.201600064.
[24] X. Zhao, M. Zhang, D. Wei, Y. Wang, S. Yan, M. Liu, X. Yang, K. Yang, H.-L. Cui, W. Fu, Label-free sensing of the binding state of MUC1 peptide and anti-MUC1 aptamer solution in fluidic chip by terahertz spectroscopy, Biomed. Opt. Express 8 (10) (2017) 4427–4437, https://doi.org/10.1364/boe.8.004427.
[25] S. Alfihed, M.H. Bergen, J.F. Holzman, I.G. Foulds, A detailed investigation on the terahertz absorption characteristics of polydimethylsiloxane (pdms), Polymer 153 (2018) 325–330, https://doi.org/10.1016/j.polymer.2018.08.025.
[26] H.S. Salapare, F. Guittard, X. Noblin, E. Taffin de Givenchy, F. Celestini, H. J. Ramos, Stability of the hydrophilic and superhydrophobic properties of oxygen plasma-treated poly(tetrafluoroethylene) surfaces, J. Colloid Interface Sci. 396 (2013) 287–292, https://doi.org/10.1016/j.jcis.2012.12.072.
[27] S. Zanini, R. Barni, R.D. Pergola, C. Riccardi, Modification of the PTFE wettability by oxygen plasma treatments: influence of the operating parameters and investigation of the ageing behaviour, J. Phys. D: Appl. Phys. 47 (32) (2014), 325202, https://doi.org/10.1088/00223727/47/32/325202.
[28] J. Nakamatsu, L.F. Delgado-Aparicio, R.D. Silva, F. Soberon, Ageing of plasma-treated poly(tetrafluoroethylene) surfaces, J. Adhes. Sci. Technol. 13 (7) (1999) 753–761, https://doi.org/10.1163/156856199×00983.
[29] D.J. Wilson, R.L. Williams, R.C. Pond, Plasma modification of PTFE surfaces – Part I: surfaces immediately following plasma treatment, Surf. Interface Anal. 31 (5) (2001) 385–396, https://doi.org/10.1002/sia.1065.
[30] J. Ryu, K. Kim, J. Park, B.G. Hwang, Y. Ko, H. Kim, J. Han, E. Seo, Y. Park, S.J. Lee, Nearly perfect durable superhydrophobic surfaces fabricated by a simple one-step plasma treatment, Sci. Rep. 7 (1) (2017) 1981, https://doi.org/10.1038/s41598-017-02108-1.
[31] P.U. Jepsen, U. Møller, H. Merbold, Investigation of aqueous alcohol and sugar solutions with reflection terahertz time-domain spectroscopy, Opt. Express 15 (22) (2007) 14717–14737, https://doi.org/10.1364/oe.15.014717.
[32] L. Afsah-Hejri, P. Hajeb, P. Ara, R.J. Ehsani, A comprehensive review on food applications of terahertz spectroscopy and imaging, Compr. Rev. Food Sci. Food Saf. 18 (2019) 1563–1621, https://doi.org/10.1111/1541-4337.12490.
[33] P. Lam, K.J. Wynne, G.E. Wnek, Surface-tension-confined microfluidics, Langmuir 18 (3) (2002) 948–951, https://doi.org/10.1021/la010589v.
[34] J. West, A. Michels, S. Kittel, P. Jacob, J. Franzke, Microplasma writing for surface-directed millifluidics, Lab Chip 7 (2007) 981–983, https://doi.org/10.1039/B706788G.
[35] S. Bouaidat, O. Hansen, H. Bruus, C. Berendsen, N.K. Bau-Madsen, P. Thomsen, A. Wolff, J. Jonsmann, Surface-directed capillary system; theory, experiments and applications, Lab Chip 5 (8) (2005) 827–836, https://doi.org/10.1039/b502207j.
[36] B. Zhao, J.S. Moore, D.J. Beebe, Surface-directed liquid flow inside microchannels, Science 291 (5506) (2001) 1023–1026, https://doi.org/10.1126/science.291.5506.1023.
[37] A. Hibara, S. Iwayama, S. Matsuoka, M. Ueno, Y. Kikutani, M. Tokeshi, T. Kitamori, Surface modification method of microchannels for gasliquid two-phase flow in microchips, Anal. Chem. 77 (3) (2005) 943–947, https://doi.org/10.1021/ac0490088.
[38] H. Bruus, Theoretical Microfluidics, 18, Oxford University Press, Oxford, 2008.
[39] J.W. Bye, S. Meliga, D. Ferachou, G. Cinque, J.A. Zeitler, R.J. Falconer, Analysis of the hydration water around bovine serum albumin using terahertz coherent synchrotron radiation, J. Phys. Chem. A 118 (1) (2014) 83–88, https://doi.org/10.1021/jp407410g.
[40] J. Xu, K.W. Plaxco, S.J. Allen, Absorption spectra of liquid water and aqueous buffers between 0.3 and 3.72 THz, J. Chem. Phys. 124 (3) (2006), 036101, https://doi.org/10.1063/1.2151267.
[41] S. Yadav, S. Shire, D. Kalonia, Viscosity analysis of high concentration bovine serum albumin aqueous solutions, Pharm. Res. 28 (2011) 1973–1983, https://doi.org/10.1007/s11095-011-0424-7.
[42] S. McClellan, E. Franses, Effect of concentration and denaturation on adsorption and surface tension of bovine serum albumin, Colloids Surf. B: Biointerfaces 28 (2003) 63–75, https://doi.org/10.1016/S09277765(02)00131-5.
[43] D.J. Wilson, R.L. Williams, R.C. Pond, Plasma modification of PTFE surfaces – Part II: plasma-treated surfaces following storage in air or PBS, Surf. Interface Anal. 31 (5) (2001) 397–408, https://doi.org/10.1002/sia.1066.
[44] B.D. Cassie, Wettability of porous surfaces, Trans. Faraday Soc. 5 (1944) 546–551.
[45] D.J. Rowe, A. Porch, D.A. Barrow, C.J. Allender, Microfluidic device for compositional analysis of solvent systems at microwave frequencies, Sens. Actuators B: Chem. 169 (2012) 213–221, https://doi.org/10.1016/j.snb.2012.04.069.

**Nicholas Klokkou** received his MPhys in Physics at the University of Southampton in 2016, where he is now pursuing a Ph.D. with the Terahertz Laboratories and the Integrated Photonic Devices group. His research interests are in combining microfluidic devices with terahertz time-domain spectroscopy, to investigate protein hydration dynamics, along with further developing frequency dependent complex refractive index extraction techniques through iterative algorithms and machine learning, for sample characterisation.

**David Rowe** is a research fellow with the Mid-Infrared Silicon Photonics Group as part of the Zepler Institute at the University of Southampton. His research interests are in translating novel photonics into lab-on-a-chip devices for biomedical applications, particularly mid-infrared spectroscopy for point-of-care diagnostics. He received his BEng in Electronic Engineering from Cardiff University in 2009 and later completed his Ph.D. ('Microfluidic microwave resonant sensors') in 2012. He has received various awards including the 2011 Institute of Physics Mansel Davies award and was nominated for a Vice Chancellor's Award in 2019 for his work on equality and diversity.

**Bethany Bowden** received her MChem in Chemistry from Cardiff University in 2018 and is now pursuing a Ph.D. as part of the Electrochemistry group at the University of Southampton. Her research interests are in waveguide enhanced Raman spectroscopy and the modification of tantalum pentoxide surfaces to optimise their functionality and stability, such as to promote binding of specific species in the analyte medium.

**Neil Sessions** graduated in Chemistry from the University of Exeter, UK, in 1998. He joined the Optoelectronics Research Centre at Southampton University in 2000 working on soft glass optical fibre fabrication and on integrated photonic materials and devices. He now manages the Zepler Institute's Integrated Photonics Cleanroom.

**Jonathan West** received a Ph.D. in Biosensors and Microfluidics in 2003 from the National Microelectronics Research Centre (now Tyndall Institute) in Cork, Ireland, then worked on technology commercialization at INEX in Newcastle. He moved to ISAS, Dortmund, Germany, to establish his microfluidics for cell biology research theme and is now a lecturer in Biomedical Microfluidics at the University of Southampton. His lab is focused on microfluidic innovation for biological discovery *en route* to clinical translation.

**James Wilkinson** is Professor of Optoelectronics in Southampton University's Optoelectronics Research Centre, of which he is a founder-member. He took his BSc and Ph.D., both in electronic engineering, from University College London in 1977 and 1985. He conducted research into optical fibre systems at the GEC Hirst Research Centre, London, from 1977 to 1979, and into optical monitoring and control for haemodialysis procedures at St Bartholomew's Hospital, London, between 1983 and 1985. His research focusses on optical materials and devices for sensing and telecommunications. James is a Fellow of the IEEE, IET and the IoP and was a cofounder of UoS spin-out Mesophotonics Ltd, which commercialised Klarite SERS chips. From 2014 to 2018 he was Associate Dean, Planning and Strategy, for the Faculty of Physical Sciences and Engineering at Southampton.

**Vasilis Apostolopoulos** received his Ph.D. degree at the University of Southampton in 2003 where he is now an associate professor. He has worked at the University of Cambridge and the Ecole Polytechnique de Lausanne. He is interested in developing THz time domain spectroscopy and its interface with optical systems such as integrated optics, metamaterial devices and microfluidics. He is also interested in Laser sources, specifically vertical external surface emitting lasers and their applications for nonlinear processes such as generation of Kerr micro-combs.